Available online at www.sciencedirect.com
SCIENCE DIRECT®
Cold Regions Science and Technology 38 (2004) 1–15
cold regions science and technology
www.elsevier.com/locate/coldregions

A numerical model for surface energy balance and thermal regime of the active layer and permafrost containing unfrozen water

Feng Ling[a,b,*], Tingjun Zhang[a]

[a] National Snow and Ice Data Center, Cooperative Institute for Research in Environmental Sciences, University of Colorado, Boulder, CO 80309-0449, USA
[b] Department of Computer Science and Technology, Zhaoqing University, Zhaoqing, Guangdong 526061, PR China

Received 16 September 2002; accepted 10 May 2003

Abstract

This paper describes a surface energy balance approach-based one-dimensional heat transfer model for estimating surface energy balance components and the thermal regime of soil. The surface energy balance equation was used to estimate the upper boundary temperature conditions for thermal conduction calculations and to calculate surface heat fluxes. The influence of unfrozen water on the thermal properties of soils was accounted for in the heat transfer model. The effect of snow was included in the model by extending the heat conduction solution into the snow layer and computing the surface heat balance components and the snow surface temperature. The model was driven by meteorological data collected at Barrow, AK, and was validated against the observed ground temperatures at Barrow. The results show good agreement between the simulated and the measured soil temperatures at depths of 0.01, 0.29, 0.50, and 1.0 m. When snow cover was present, snow surface temperatures were colder than ground surface temperatures and air temperatures, with mean temperature differences of − 5.36 and − 1.55 °C, respectively. We conclude that the model presented in this study can be used to calculate the surface energy balance components, simulate the ground temperatures, and investigate the impact of seasonal snow cover on the thermal regime of the active layer and permafrost containing unfrozen water with a quite reasonable accuracy. Snow density, which determines the snow thermal conductivity, volumetric heat capacity, and albedo in this model, can strongly affect the performance of this model.

Keywords: Surface energy balance; Permafrost; Snow cover; Unfrozen water; Modeling; Alaskan Arctic

1. Introduction

Accurate simulation of the thermal regime of the active layer and permafrost is an important component in the prediction of global changes and a prerequisite for engineering designs and constructions in cold regions. This is because nearly all physical, biological, and chemical processes occur on or within the active layer (Hinzman et al., 1991, 1998; Kane et al., 1991), and because variations in permafrost temperature can affect the ability of permafrost to support a load, seriously affecting the performance of structures constructed in permafrost regions (Johnston and Brown, 1964; Miller, 1979; Esch and Osterkamp, 1990; Lunar-

* Corresponding author. National Snow and Ice Data Center, Cooperative Institute for Research in Environmental Sciences, University of Colorado, Boulder, CO 80309-0449, USA. Tel.: +1-303-492-5562; fax: +1-303-492-2468.
E-mail address: lingf@kryos.colorado.edu (F. Ling).

0165-232X/$ - see front matter © 2004 Elsevier B.V. All rights reserved.
doi:10.1016/S0165-232X(03)00057-0

dini, 1996). It is almost impossible to analytically determine the thermal response of the active layer and permafrost to climate change, because the rate and magnitude of the thermal response of the ground to climate change are time- and temperature-dependent due to changing boundary conditions. Numerical modeling is generally regarded as the best method to accurately simulate and forecast the thermal regime of the active layer and permafrost (Miller, 1979; Kane et al., 1991).

Surface energy balance in cold regions is a complex function of seasonal snow cover, vegetation, atmospheric radiation, surface moisture content, and atmospheric temperature (Lunardini, 1981). Therefore, an accurate method for describing ground surface temperature should use physically based models that account for the relevant processes occurring within, and at the boundaries of permafrost, snow, and atmospheric components of the natural system. The surface energy balance approach is a reasonable method of establishing surface temperature boundary conditions because it tends to preserve the cause and effect relationship between surface temperatures and heat fluxes (Miller, 1979).

Seasonal snow cover, which presents a barrier to heat loss from the ground to the air in winter, is a leading factor in ground thermal regime and active layer depth (Lachenbruch, 1959; Outcalt et al., 1975; Goodrich, 1982; Williams and Smith, 1989; Zhang et al., 1996; Romanovsky and Osterkamp, 2000; Taras et al., 2002). Snow has a high surface albedo and high emissivity, which cool the snow surface, while snow cover has a low thermal conductivity, which makes it a good insulator. Melting snow is also a heat sink owing to the latent heat of fusion. Thus, an efficient model of heat transfer with phase change for permafrost must include the effect of seasonal snow cover.

Freezing or thawing occurs in permafrost results in a partially frozen system consisting of soil, air, ice, and unfrozen water coexisting in thermal equilibrium. Due to the presence of unfrozen water in permafrost, the phase change between water and ice in soil occurs gradually over a temperature range below the freezing temperature. It has been understood theoretically for many years that unfrozen water strongly influences heat and mass transport processes in soils (Williams, 1964; Nakano and Brown, 1971; Anderson, 1973; Harlan, 1973; Jame and Norum, 1980; Inaba, 1983; Civan and Sliepcevich, 1985; Osterkamp, 1987; Civan, 2000). Failure to take the effect of unfrozen water into account when modeling thermal regime of permafrost will produce large errors (Romanovsky and Osterkamp, 2000; Riseborough, 2002).

The most widely used upper boundary condition for numerical studies of the effect of seasonal snow cover on the thermal regime of the active layer and permafrost is temperature boundary conditions (e.g., Lachenbruch, 1959; Goodrich, 1982; Zhang et al., 1996; Zhang and Stamnes, 1998). They have also been used, but relatively fewer in number, for simulating the permafrost thermal regime using the surface energy balance approach to estimate surface temperature conditions. Several surface energy balance models, which are forced with daily weather information, have been developed and used to simulate the snowmelt and tundra soil thermal regime (Outcalt et al., 1975; Miller, 1979), and to investigate the effect of tundra vegetation and climate change on ground temperature (Ng and Miller, 1977; Smith and Riseborough, 1983). However, these models do not include the effect of unfrozen water on soil thermal properties. Hinzman et al. (1998) developed a spatially distributed surface energy balance model for calculating soil temperature profiles and thaw depth in permafrost regions. The model performs quite well with 1-day time increments, but seasonal snow cover was not included in the model.

The purpose of this paper is to describe a one-dimensional finite difference model with phase change for surface energy balance and thermal regime of the active layer and permafrost containing unfrozen water. A surface energy balance equation for lake ice evolution (Liston and Hall, 1995) was used to estimate the upper boundary condition for thermal conduction calculations. The influence of unfrozen water on the physical and thermal properties of permafrost was accounted for in the heat transfer model based on a model described by Osterkamp (1987). The effect of snow was included in the model by extending the heat conduction solution into the snow layer and computing the surface heat balance and the snow surface temperature. The model was validated against field measurement collected at Barrow, AK. The outputs of the validated model, surface temperatures, surface energy balance components, and mean annual ground temperature with depth are discussed.

2. Surface energy balance model

Ground surface energy balance is driven by the net flux of heat arising from absorbed solar and thermal radiation, and from sensible and latent heat transfer between the ground and the overlaying air. Mathematically, this takes the following form:

$$(1-\alpha)Q_{si}+Q_{li}+Q_{le}+Q_h+Q_e+Q_c=Q_m \quad (1)$$

where α is the albedo of the surface, Q_{si} is the solar radiation reaching the surface of the earth, Q_{li} is the incoming longwave radiation, Q_{le} is the emitted longwave radiation, Q_h is the turbulent exchange of sensible heat, Q_e is the turbulent exchange of latent heat, Q_c is the conduction heat flux through the snow cover or ground surface from below, and Q_m is the energy flux available for melting. Each component of the energy term, Q, has unit of W m^{-2}.

The incoming longwave radiation is given by the empirical description (Satterlund, 1979; Fleagle and Businger, 1980)

$$Q_{li}=1.08\left(1-\exp\left(-(0.01e_a)^{\frac{T_a}{2016}}\right)\right)\sigma T_a^4 \quad (2)$$

$$\log_{10}e_a=11.40-\frac{2353}{T_{dp}} \quad (3)$$

where T_a is mean daily air temperature (°K), T_{dp} is daily dew-point temperature (K), σ is the Stefan–Boltzmann constant (W m^{-2} K^{-4}), and e_a is atmospheric vapor pressure (Pa).

The emitted longwave radiation is given by

$$Q_{le}=-\varepsilon_s\sigma T_{s0}^4 \quad (4)$$

where ε_s is the surface emissivity, T_{s0} is ground surface or snow surface temperature (K).

The turbulent exchange of sensible and latent heat, Q_h and Q_e, are given by Price and Dunne (1976):

$$Q_h=\rho_a C_p D_h \zeta (T_a-T_{s0}) \quad (5)$$

$$Q_e=\rho_a L_s D_e \zeta\left(0.622\frac{e_a-e_{s0}}{P_a}\right) \quad (6)$$

The exchange coefficients for sensible heat and latent heat, D_h and D_e, and the stability function, ζ, are

$$D_h=D_e=\frac{\kappa^2 U_s}{(\ln(z/z_0))^2} \quad (7)$$

$$\zeta=\frac{1}{(1+10R_i)} \quad (8)$$

where ρ_a is the density of the air (kg m^{-3}), assumed to be 1.275 kg m^{-3}, C_p is the specific heat of air (J K^{-1} kg^{-1}), assumed to be 1004.0 J K^{-1} kg^{-1}, e_{s0} is the vapor pressure of the surface (Pa), P_a is atmospheric pressure (Pa), L_s is the latent heat of sublimation (J kg^{-1}), κ is Von Karman's constant, U_s is the wind speed (m s^{-1}) at reference height z (m), and z_0 is the roughness length (m).

The Richardson number, R_i, is given by

$$R_i=\frac{gz(T_a-T_{s0})}{T_a U_z^2} \quad (9)$$

where g is the gravitational acceleration (m s^{-2}).

Heat conducted through the snow and ground is (Liston and Hall, 1995)

$$Q_c=-(T_{s0}-T_b)\left(\frac{z_s}{k_s}+\frac{z_g}{k_g}\right)^{-1} \quad (10)$$

where T_b is the ground temperature at the bottom of top layer (°K), z_s and z_g are the thicknesses of snow and the top layer of ground (m), respectively, and k_s and k_g are the thermal conductivities of the snow and ground (W m^{-1} K^{-1}), respectively.

The surface energy balance model was forced with daily meteorological data and was solved iteratively for the surface temperature, T_{s0}, using the Newton–Raphson method

$$T_{s0}^{n+1}=T_{s0}^n-\frac{f(T_{s0})}{f'(T_{s0})} \quad (11)$$

where $f(T_{s0})$ takes the following form:

$$f(T_{s0})=(1-\alpha_s)Q_{si}+Q_{li}+Q_{le}(T_{s0})+Q_h(T_{s0})+Q_e(T_{s0})+Q_c(T_{s0})=0. \quad (12)$$

3. Heat transfer model

It is assumed that unfrozen water does not move within permafrost. Then the one-dimensional heat transfer equation can be written as

$$C\frac{\partial T}{\partial t}=\frac{\partial}{\partial x}\left(k\frac{\partial T}{\partial x}\right) \tag{13}$$

$$C=C_{\mathrm{v}}+L\frac{\partial \vartheta_{\mathrm{u}}}{\partial T} \tag{14}$$

$$\vartheta_{\mathrm{u}}=\frac{\rho_{\mathrm{b}}}{\rho_{\mathrm{u}}}a\,|\,T\,|^{b} \tag{15}$$

where T is soil temperature (°C), k is thermal conductivity (W m^{-1} °C^{-1}), C and C_{v} are the apparent volumetric heat capacity and volumetric heat capacity of soil (J m^{-3} °C^{-1}), respectively, t is time (day), L is the volumetric latent heat of fusion for ice (J m^{-3}), θ_{u} is the volumetric unfrozen water content, ρ_{b} and ρ_{u} are the dry bulk density of permafrost and density of unfrozen water, respectively, a and b are empirically derived material-dependent constants.

By assuming a saturated system, the thermal conductivity and the volumetric heat capacity for a mixture of soil particles, unfrozen water, and ice are represented as

$$k=k_{\mathrm{s}}^{\vartheta_{\mathrm{s}}}k_{\mathrm{u}}^{\vartheta_{\mathrm{u}}}k_{\mathrm{i}}^{\vartheta_{\mathrm{i}}} \tag{16}$$

$$C_{\mathrm{v}}=\vartheta_{\mathrm{s}}C_{\mathrm{s}}+\vartheta_{\mathrm{u}}C'_{\mathrm{u}}+\vartheta_{\mathrm{i}}C_{\mathrm{i}} \tag{17}$$

$$\vartheta_{\mathrm{s}}+\vartheta_{\mathrm{i}}+\vartheta_{\mathrm{u}}=1 \tag{18}$$

where subscripts s, u, and i refer to soil particle, unfrozen water, and ice.

The latent heat of freezing of water, L, and the temperature-dependent thermal properties k_{u}, k_{i}, C_{u}, and C_{i} are (Osterkamp, 1987)

$$L=\rho_{\mathrm{u}}(333.2+4.995T+0.02987T^{2}) \tag{19}$$

$$k_{\mathrm{u}}=0.11455+1.6318\times10^{-3}(273.15+T) \tag{20}$$

$$k_{\mathrm{i}}=0.4685+\frac{488.19}{273.15+T} \tag{21}$$

$$C_{\mathrm{u}}=4.20843+1.11362\times10^{-1}T+5.12142\times10^{-3}T^{2}+9.3482\times10^{-5}T^{3} \tag{22}$$

$$C_{\mathrm{i}}=1.94+7.14\times10^{-3}T \tag{23}$$

The thermal properties of soil particles, k_{s} and C_{s}, are determined by the type of soil.

The heat transfer model was solved using an implicit finite difference scheme with the time step of 1 day. The upper boundary was set at the snow surface when seasonal snow cover was present and at ground surface when the snow cover was absent. The lower boundary was set at a specific depth with a constant heat flux or constant temperature as lower boundary condition.

4. Results

The model was validated with meteorological data collected at Barrow, AK, where ground temperatures at depths of 0.01, 0.29, 0.5 and 1.0 m are also available (Hinkel, 2002). The root mean square deviation of the calculated ground temperature from the measured ground temperature was used to evaluate the validity of the physical and thermal parameter calibration and the model performance. The deviation was defined by

$$D_{\mathrm{rms}}=\left[\frac{\sum_{i=1}^{N}(T_i^{\mathrm{c}}-T_i^{\mathrm{m}})^{2}}{N-1}\right]^{1/2} \tag{24}$$

where T^{c} is the calculated mean daily temperature, T^{m} is the measured mean daily temperature, and N is the total number of data points.

4.1. Calibration of the heat transfer model

The heat transfer model was calibrated using measured ground temperature data from 1 July 1995 to 31 December 1998. Based on Barrow soil conditions (Nakano and Brown, 1972; McGaw et al., 1978; Hinkel, 1997; Romanovsky and Osterkamp, 2000), the analysis domain was assumed to consist of four major soil types: peat layer (0.0–0.16 m), silt A layer (0.16–0.35 m), silt B layer (0.35–5.0 m), and silt C layer (5.0–35.0 m). Soils were divided into 361 layers with layer thickness, Δx, ranging from 0.03 to 0.1 m. The upper boundary was set at a depth of 0.01 m, with the measured mean daily ground temperatures as upper boundary condition (Fig. 1). The lower

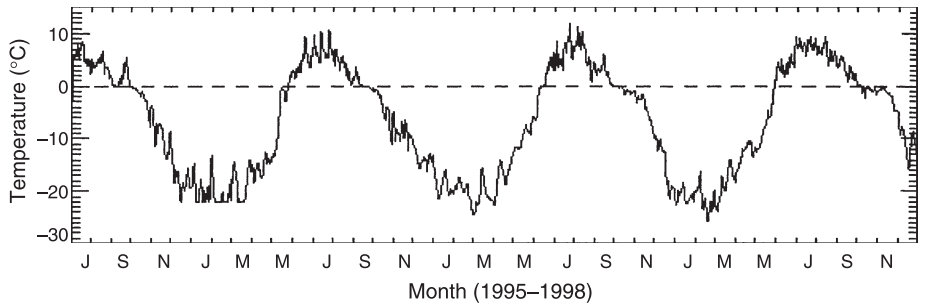

Fig. 1. Measured mean daily soil temperature at a depth of 0.01 m from July 1995 through December 1998 at Barrow, AK. This is the upper boundary condition for heat transfer model calibration.

boundary was located at 35 m, which is sufficiently deep to ensure no significant effect on temperatures at shallow depths. At the lower boundary, there was a constant geothermal heat flux of -0.0565 W m^{-2} (Lachenbruch et al., 1982)

$$k\frac{\partial T(t)}{\partial x} = 0.0565 \text{ W m}^{-2} \quad (25)$$

The volumetric heat capacities for peat particles, C_p, and silt particles C_s, are given by (Kay and Goit, 1975)

$$C_p = -0.1333 + 6.255 \times 10^{-3}(273.15 + T) \quad (26)$$

$$C_s = 0.4091 + 5.433 \times 10^{-3}(273.15 + T) \quad (27)$$

The thermal conductivities of peat particles and silt particles are 0.25 and 2.92 W m^{-1} °C^{-1} (Williams and Smith, 1989), respectively. The parameters of unfrozen water content for peat, silts A, B, and C, described in Eq. (15), were derived from Romanovsky and Osterkamp (2000). The volumetric water content for peat, silts A, B, and C were found by fitting the calculated ground temperatures at depths of 0.29, 0.5, and 1.0 m to the observed values using the trial and error method. The calibrated physical properties for various type of soils are summarized in Table 1. The corresponding variations of volumetric unfrozen water content with temperature and thermal properties with temperature are presented in Figs. 2 and 3, respectively.

Table 1
Summary of the calibrated physical properties of soil for the heat transfer model

Depth (m)	Soil type	Volumetric water content (%)	$(\rho_b)/(\rho_u)a$	b
0.0–0.15	Peat	66.6	2.6	−0.38
0.15–0.35	Silt A	55.5	12.0	−0.50
0.35–5.0	Silt B	52.5	6.4	−0.38
5.0–35.0	Silt C	39.2	3.6	−0.30

Initially, the soil temperature of each node was interpolated using the mean annual permafrost surface temperature of -9.0 °C (Lachenbruch and Marshall, 1969) and the lower boundary condition in Eq. (25). The heat transfer model was run starting with the measured upper boundary temperature on 1 July 1995, until the soil temperature profile reached equilibrium with the upper and lower boundary conditions, ensuring that the initial temperature condition did not influence results. Then, the equilibrium temperature profile was used as the initial condition, and the measured average daily ground temperatures from 2 July 1995 through 31 December 1998 were used to

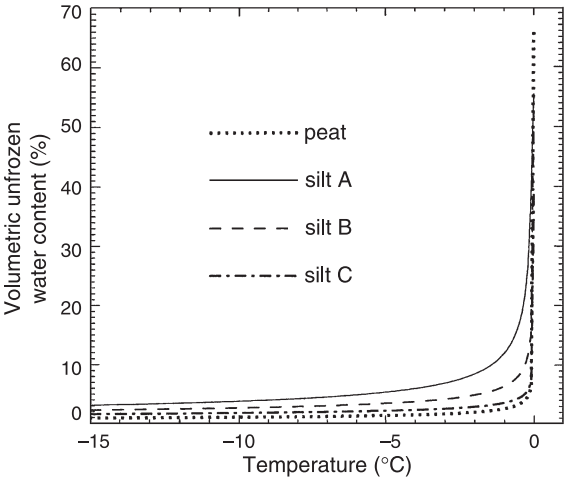

Fig. 2. Variations of volumetric unfrozen water content with temperature for different soils used in this study.

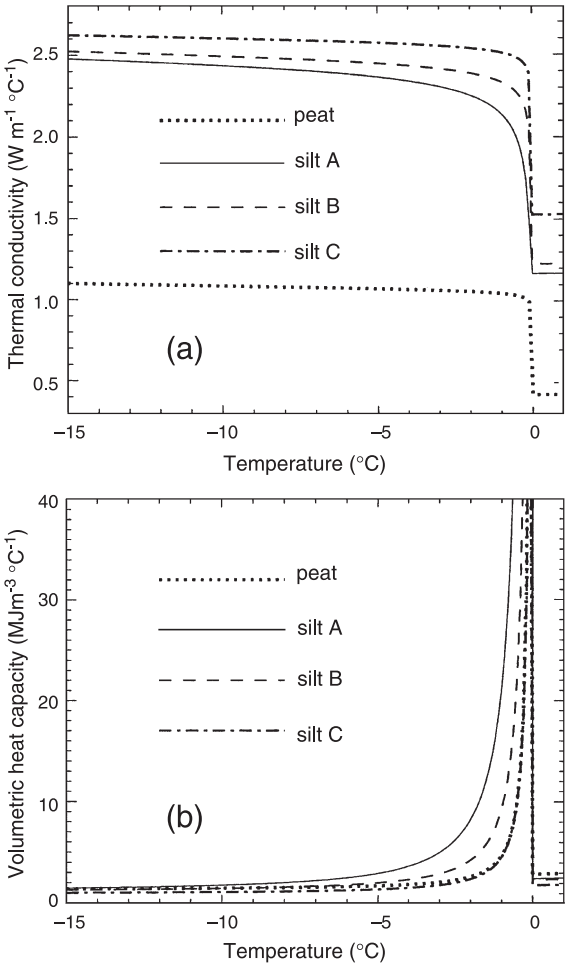

Fig. 3. Variations of (a) thermal conductivity and (b) apparent volumetric capacity with temperature for different soils.

drive the model, with a time step of 1 day. The equilibrium condition is determined when the maximum difference of soil temperatures at all levels between two successive time steps was less than 0.001 °C.

Fig. 4 shows a comparison between the simulated and measured ground temperatures in the active layer (Fig. 4a), near the permafrost surface (Fig. 4b), and in shallow permafrost (Fig. 4c) from 1996 through 1998. The simulated and measured permafrost temperatures at depths of 0.29, 0.50, and 1.0 m agree well. The root mean square deviation of the calculated ground temperatures from the measured values is less than 0.5 °C in all cases (Table 2). This suggests that the physical and thermal parameters used in the heat transfer model are reasonably accurate. It should be noted, however, that the simulated ground temperatures at a depth of 0.29 m were lower than the measured values by at most 1.5 °C during the soil thawing period each year (Fig. 4a). This systematic bias can be attributed to the nonconductive heat transfer of the convection (Kane et al., 1991, 2001), which is not included in the heat transfer model. During the soil thawing period, the infiltration of snow melt water and rainfall increases the soil temperature sooner than the model would predict, as has been observed in field studies at Barrow (Hinkel et al., 2001). Convective heat transfer becomes progressively more important as the soil warms and remains unfrozen longer. As a result, the model will slightly underpredict soil temperatures. However, the amount of under-prediction is relatively small and the estimate of thaw depths will not be grossly in error (Kane et al., 1991, 2001), as can be seen in Fig. 4b and c.

4.2. Model validation

After calibration, the heat transfer model was combined with the surface energy balance model. The coupled model was validated using the ground temperatures collected at Barrow between July 1997 and June 1998, with inputs of mean daily air temperature, dewpoint temperature, incident solar radiation, wind speed, seasonal snow cover thickness, and atmospheric pressure measured at Barrow, AK (Fig. 5). The upper boundary was set at the snow surface when the seasonal snow cover was present and at the ground surface when the seasonal snow cover was absent.

Snow cover was treated as several equal adherent layers, and the number of layers, N_{snow}, was determined by the snow thickness:

$$N_{\text{snow}} = \begin{cases} 1 & 0 < H_{\text{snow}} \le 0.07 \\ 2 & 0.07 < H_{\text{snow}} \le 0.15 \\ 3 & 0.15 < H_{\text{snow}} < 0.24 \\ 4 & 0.24 < H_{\text{snow}} \le 0.35 \\ 5 & 0.35 < H_{\text{snow}} \end{cases} \quad (28)$$

where H_{snow} is the thickness of snow cover (m).

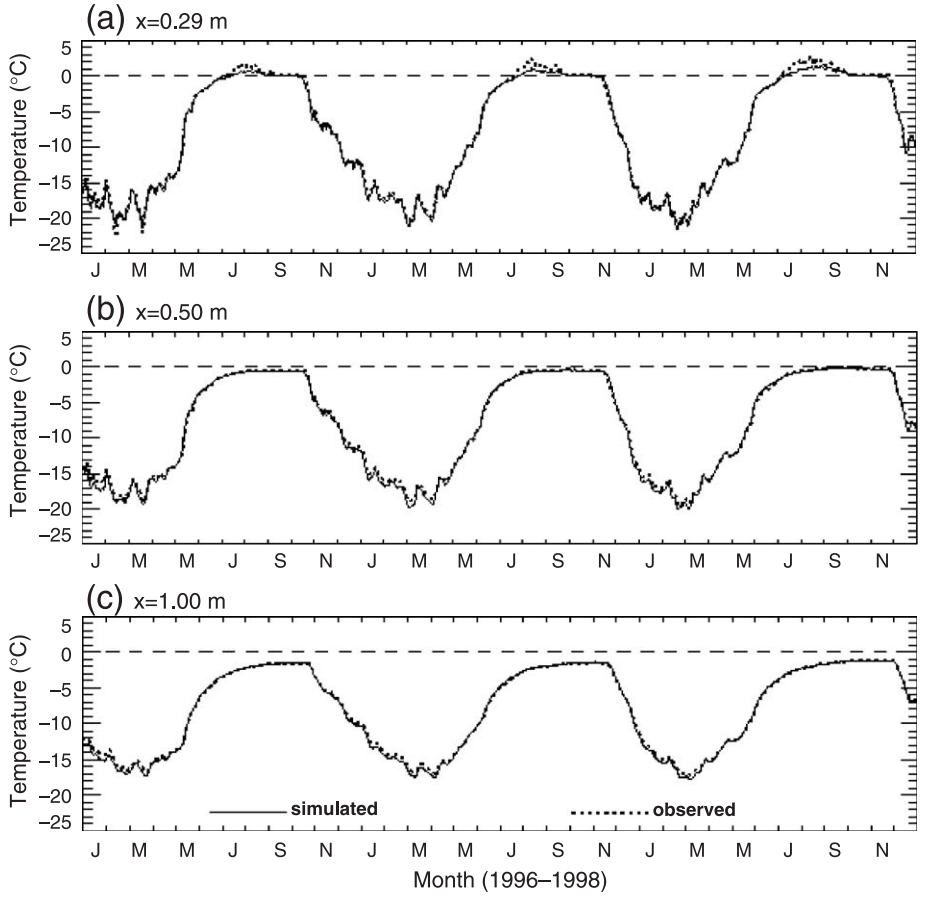

Fig. 4. A comparison between simulated and measured ground temperatures at depths of (a) 0.29 m; (b) 0.5 m, and (c) 1.0 m for the calibration period of 1996 through 1998.

The effective thermal conductivity and the volumetric heat capacity of snow were related to snow density using empirical formulas (Goodrich, 1982):

$$k_{\text{snow}} = 2.9 \times 10^{-6} \rho_{\text{snow}}^2 \tag{29}$$

$$C_{\text{snow}} = 2.09 \times 10^{3} \rho_{\text{snow}} \tag{30}$$

where ρ_{snow} is the density of snow (kg m^{-3}).

The albedo of snow, α_s, decreases with increasing of snow density, ρ_{snow} (Anderson, 1976):

$$\alpha_s = \begin{cases} 1.0 - 0.247[0.16 + 110(\rho_s/1000)^4]^{1/2} & 50 \le \rho_s \le 450 \\ 0.6 - \rho_s/4600 & \rho_s > 450 \end{cases} \tag{31}$$

The daily albedo, roughness length, and emissivity for tundra surface at Barrow were chosen as 0.17 (Outcalt et al., 1975; Stone et al., 2002), 0.015 m (Outcalt et al., 1975), and 0.92 (Miller, 1979), respectively. The snow emissivity and roughness length were assumed to be 0.98 and 0.005 m (Liston and

Table 2
The root mean square deviation (°C) of the calculated ground temperature from the measured value for 1996 through 1998

Time (year)	Depth (m)		
	0.29	0.5	1.0
1996	0.49	0.46	0.40
1997	0.47	0.44	0.38
1998	0.47	0.39	0.32

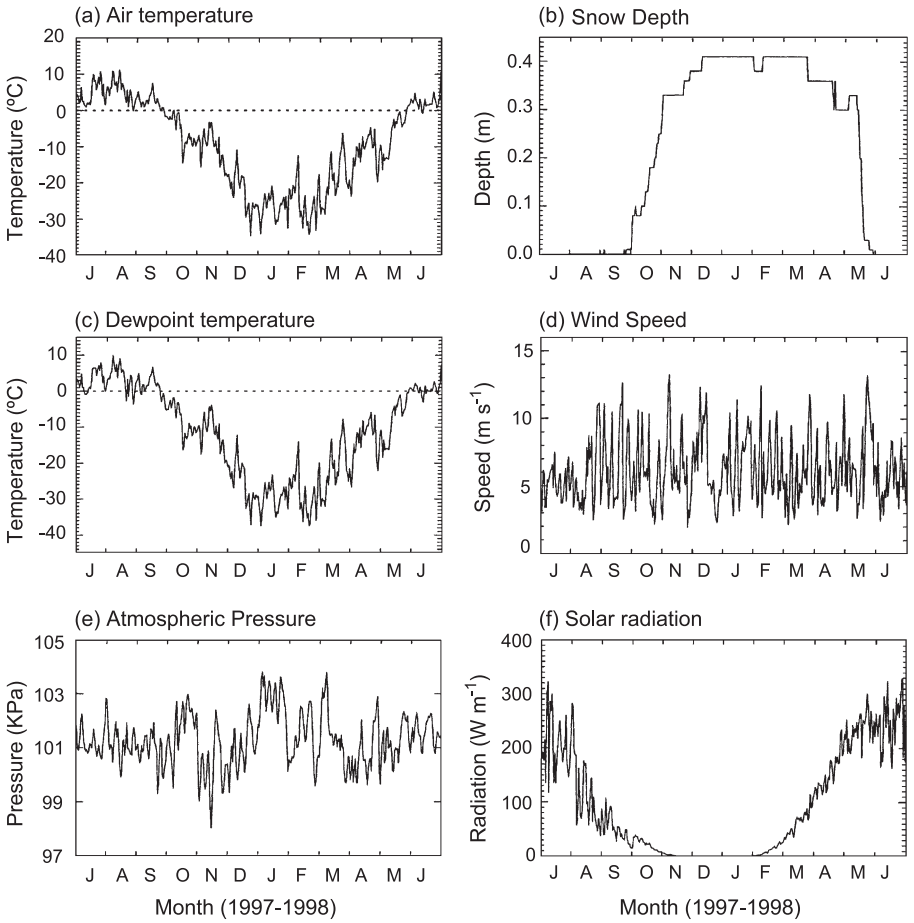

Fig. 5. Mean daily meteorological conditions measured at Barrow, AK, for the period of July 1997 to June 1998.

Hall, 1995) before snow starts to melt, and were set at 0.96 (Zhang et al., 2001) and 0.015 (Outcalt et al., 1975) during the snow melt period of 13–28 May 1998.

The calculated temperature profile on 30 June 1997 from the calibrated heat transfer model was used as the initial condition, and the surface energy balance approach was then used to evaluate the upper boundary condition in each time step of 1 day. When snow cover exists and the surface equilibrium temperature is above 0 °C, energy is available to either ripen or melt snow cover. In this case, the snow surface temperature was reset to 0 °C and the surface energy balance components and the ground temperatures were recalculated.

In the first run case (RC1), snow density was set at a constant of 270 kg m^{-3}, the corresponding snow thermal conductivity, volumetric heat capacity, and surface albedo were 0.211 W m^{-1} C^{-1}, 0.564 MJ m^{-3} $°C^{-1}$, and 0.787, respectively. Considerable discrepancies exist between the simulated and observed ground temperatures for RC1. The modeled temperatures were too cold in autumn and too warm in spring, compared with the measured values (Fig. 6). The deviation of the calculated ground temperature at a depth of 0.01 m from the measured temperature was 1.63 °C (Table 3). This is primarily due to errors in snow density. Snow density is the most important factor affecting the performance of the current model because it determines the albedo, thermal conductiv-

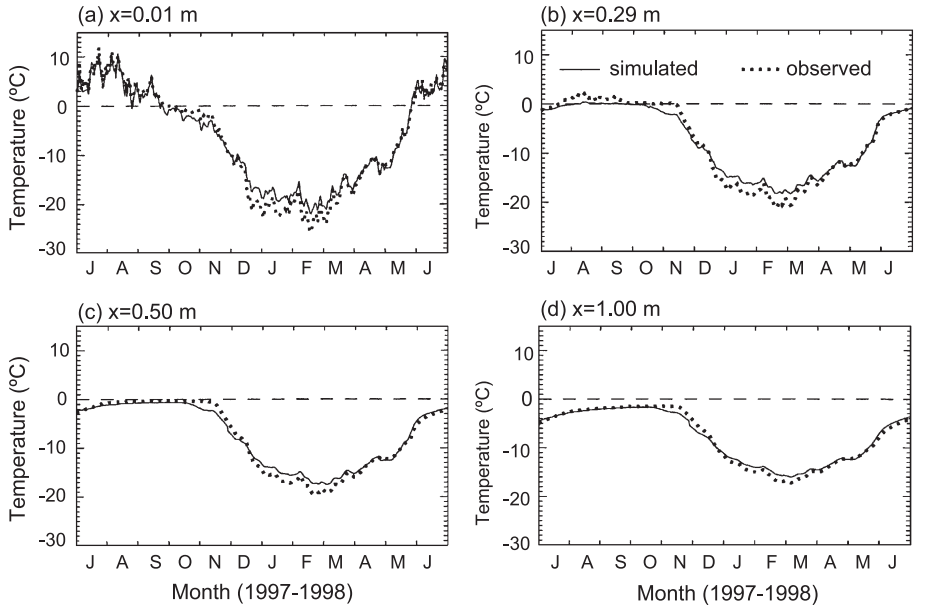

Fig. 6. A comparison between simulated and measured ground temperatures at depths of (a) 0.01 m; (b) 0.29 m; (c) 0.50 m; and (d) 1.0 m for the period of July 1997 to June 1998 for simulation RC1.

ity, and volumetric heat capacity of snow. In the Alaskan Arctic, seasonal snow cover usually consists of hard, high density, wind packed wind slab layers, with coarse, lower density depth hoar layers. The density of a wind slab layer varies from 400 to 500 kg m^{-3}, and the density of a depth hoar layer varies from 150 to 250 kg m^{-3} (Benson and Sturm, 1993; Zhang et al., 1996). Thus, the density of seasonal snow cover could vary considerably with air temperature, time, and relative humidity (Jordan, 1991; Gustafsson et al., 2001). Using a constant snow density may have resulted in the temperature difference.

In the second run case (RC2), the snow density was set at four average values according to variations of snow thickness with time (Fig. 5b). The average density values were determined when the deviations of the calculated ground temperatures from the measured values reached their minimums. The corresponding thermal conductivity, volumetric heat capacity, and albedo were derived from Eqs. (29)–(31), and are summarized in Table 4.

Table 3
Deviations (°C) of the calculated ground temperature from the measured ground temperature

Simulation case	Depth (m)			
	0.01	0.29	0.50	1.00
RC1	1.63	1.33	0.99	0.72
RC2	0.92	0.70	0.42	0.34

Table 4
Physical and thermal properties of snow cover at different periods for run case RC2

Period (day)	Mean density (kg m^{-3})	Albedo	Thermal conductivity (W m^{-1} C^{-1})	Volumetric heat capacity MJ m^{-3} $°C^{-1}$
22 September–31 October 1997	154	0.884	0.069	0.322
1 November–15 December 1997	256	0.804	0.190	0.535
16 December–14 May 1998	366	0.639	0.388	0.765
15–28 May 1998	385	0.604	0.430	0.805

The simulated soil temperatures for RC2 track the measured soil temperatures quite well at each of the four depths, for the period from July 1997 to June 1998 (Fig. 7). The deviation of the calculated ground temperature from the measured value decreases as ground depth increases from 0.01 to 1.0 m (Table 3). These results indicate that the model described in this paper can be used to simulate permafrost temperatures with confidence. Errors in the simulated permafrost temperatures from RC2 may be due to the following reasons: First, the soil temperatures were measured at the Barrow Environmental Observatory (71°18.46′N, 156°35.33′W), about 5 km east of the village of Barrow on the Arctic Coastal Plain (Hinkel et al., 2001). The meteorological data (Fig. 5a–e) were collected at the Barrow National Weather Service (NWS) station, 5 km from the Barrow Environmental Observatory, and the incident solar radiation (Fig. 5f) was measured at the National Oceanic and Atmospheric Administration (NOAA) Climate Monitoring and Diagnostics Laboratory (CMDL) Barrow Observatory, located about 2 km from the Barrow Environmental Observatory. These location differences may cause errors. Second, the ground temperature at depth of 0.01 m was calculated using a linear temperature interpolation between the two neighboring points, at depths of 0.0 and 0.03 m. Third, in addition to the effect of convective heat transfer in the active layer (Kane et al., 1991, 2002) discussed in Section 4.1, convective heat transfer in seasonal snow cover could also play a role (Sturm and Johson, 1991). This nonconductive heat transfer could effectively reduce the insulating effect of the seasonal snow cover (Stein and Kane, 1983; Hinkel et al., 1997, 2001; Kane et al., 2001). Fourth, the incoming longwave radiation was calculated by using the empirical Eq. (8), which does not account for the presence of clouds. Also, the thermal conductivity, volumetric heat capacity, and albedo were estimated using empirical descriptions (Eqs. (29)–(31)). The model performance is therefore subject to the errors of these formulae. Fifth, the time step used here is daily, rather than an hourly or a shorter time scale, due to a lack of observed data.

4.3. Modeled temperatures and surface energy balance components

Fig. 8 shows the simulated differences between snow surface temperature and ground surface temper-

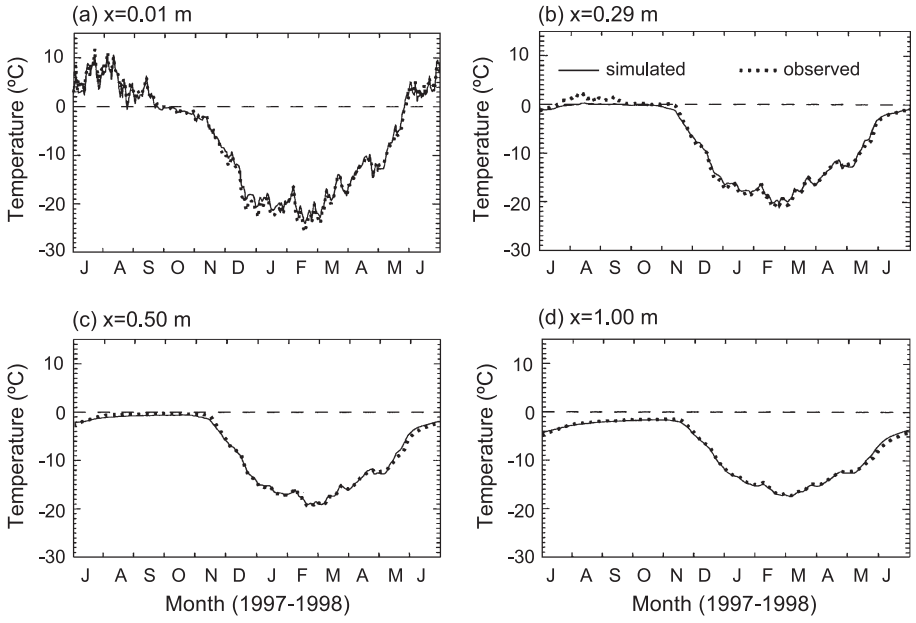

Fig. 7. A comparison between simulated and measured ground temperatures at depths of (a) 0.01 m; (b) 0.29 m; (c) 0.50 m; and (d) 1.0 m for the period of July 1997 to June 1998 for simulation RC2.

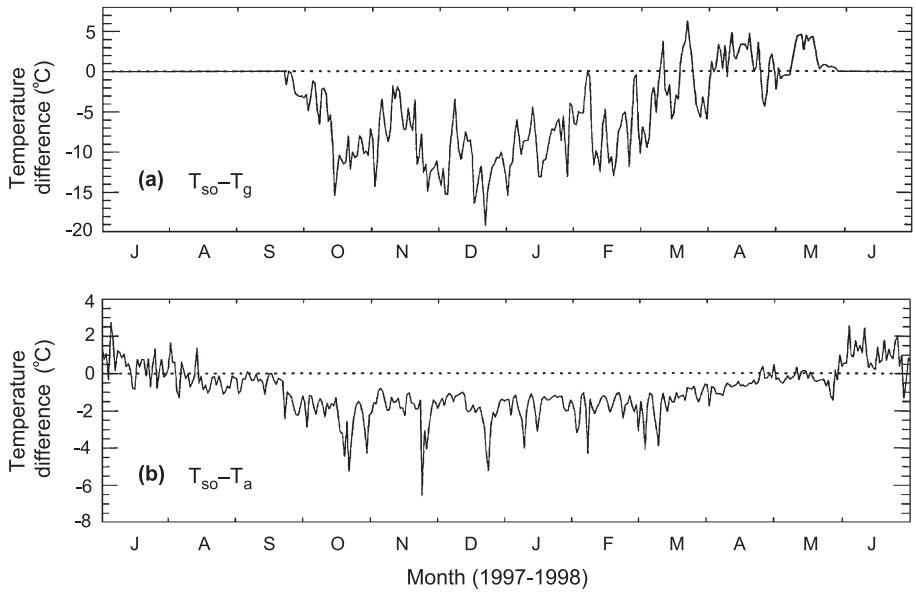

Fig. 8. Differences between (a) snow surface and ground surface temperatures and (b) snow surface and mean daily air temperatures for the period of July 1997 to June 1998 at Barrow, AK.

ature, and between snow surface temperature and mean daily air temperature, using the validated model described above (RC2). When seasonal snow cover was present, the mean daily snow surface temperatures were general colder than ground surface temperatures (Fig. 8a) and the air temperatures (Fig. 8b), with mean temperature differences of -5.36 and -1.55 °C, respectively. This is because snow has high emissivity, which causes an increase in the outgoing longwave radiation, thus cooling the snow surface. Also, snow has high surface albedo, which leads to a reduction in the absorbed solar energy, therefore lowering snow surface temperature (Weller and Holmgren, 1974). In addition, the low thermal conductivity of snow reduces the heat transfer between the snow surface and the ground surface, serving to isolate the ground from the extreme temperature changes of the air. Since heat exchange takes place at the snow surface rather than at the ground surface, the range of annual ground surface variation is reduced and ground temperatures are higher. This effect can be seen not only in winter, but also on an annual basis (Williams and Smith, 1989).

Fig. 9 shows the calculated surface energy balance components at Barrow, AK. Energy fluxes toward the ground surface were defined to be positive. The daily average net solar radiation decreased significantly as the ground surface went from snow-free to snow-covered, and increased significantly as the ground surface went from snow-covered to snow-free (Fig. 9a). This is due to the obvious difference between peat albedo and snow albedo. Similarly, the daily average net longwave radiation changed dramatically as the ground surface went from snow-free to snow-covered and snow-covered to snow-free (Fig. 9b), because of the obvious difference between peat emissivity and snow emissivity.

Because surface temperatures are warmer than the air temperature when the ground is snow-free and colder than the air temperature when the ground is snow-covered (Fig. 8b), the sensible heat flux was positive when seasonal snow cover was present and changed from positive to negative as snow cover disappeared (Fig. 9c). The latent heat flux was negative and the value was small when a stable seasonal snow cover was present between September 1997 and early May 1998, and became more negative when the active layer was in a melting or freezing period (Fig. 9d). This is generally true because the evaporation increased as the melt of

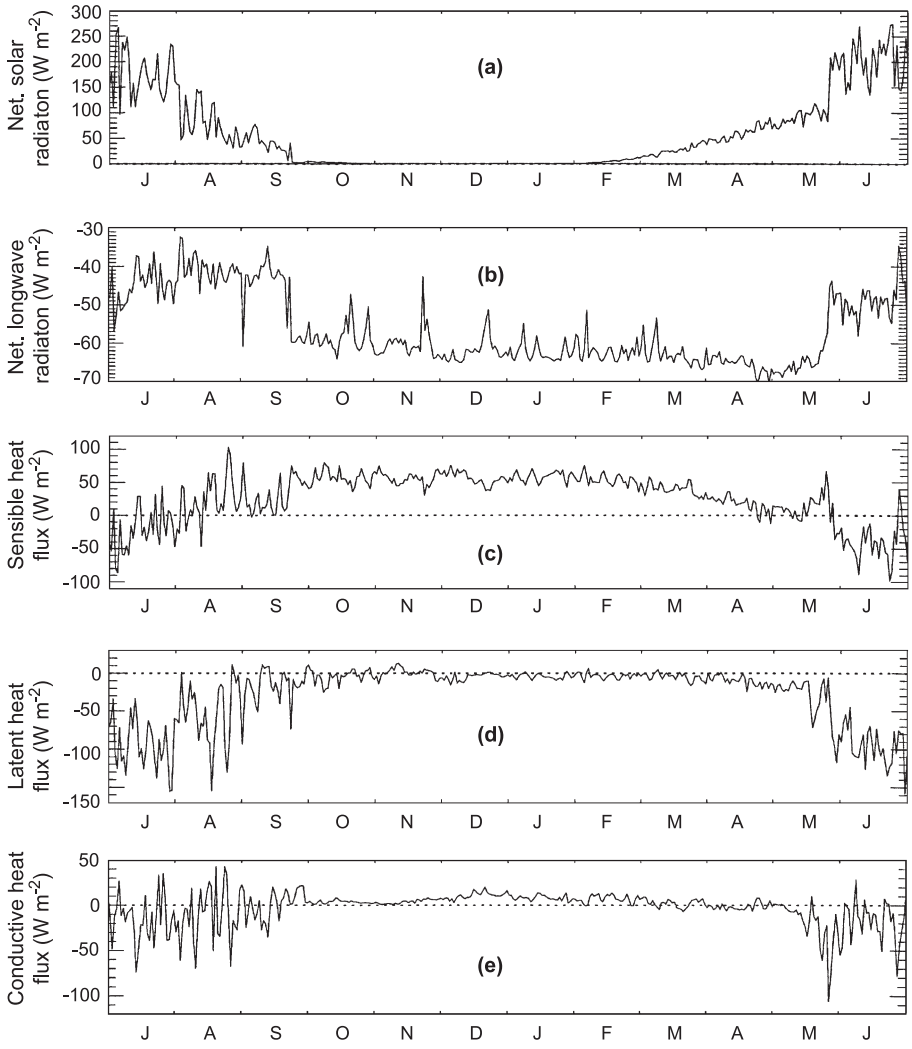

Fig. 9. Simulated surface energy balance components for the period of July 1997 to June 1998 at Barrow, AK. (a) Net solar radiation; (b) net longwave radiation; (c) sensitive heat flux; (d) latent heat flux; and (e) conductive heat flux.

snow and permafrost progressed (Liston et al., 2002).

The conductive heat flux to the atmosphere was calculated using the thermal conditions at the bottom of the top node layer, which is 0.03 m in depth. Because the ground temperature at the bottom of top node layer was generally higher than snow surface temperature when snow cover was present, and lower than the ground surface temperature when seasonal snow cover was absent, the conductive heat flux was positive when seasonal snow cover was present and negative when seasonal snow cover was absent (Fig. 9e).

Fig. 10 shows the calculated annual maximum, mean, and minimum soil temperatures with depth in 1998 at Barrow, AK. The simulated mean annual permafrost temperature at depths of 0.0, 0.5, and 1.0 m were -6.1, -7.4 and -7.6 °C, the active layer thickness was 0.44 m, and the mean permafrost temperature at 14 m depth was -8.3 °C. From field measurement at Barrow, AK (Hinkel, 2002), the mean annual ground temperatures in 1998 at depth of 0.01,

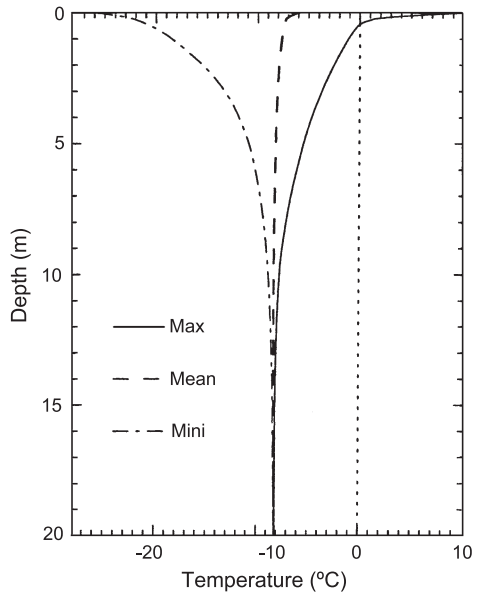

Fig. 10. Simulated annual maximum, mean, and minimum ground temperatures with depth in 1999 at Barrow, AK.

0.5, and 1.0 m were −6.1, −7.2 and −7.4 °C, the active layer thickness was 0.44 m (Hinkel et al., 2001).

5. Discussion

Snow density is a very important parameter in the model presented in this study because it determines the snow albedo, thermal conductivity, and volumetric heat capacity through empirical formulae. Therefore, systematic field observations of snow density and the accurate empirical formulae to calculate albedo, thermal conductivity, and volumetric heat capacity are needed for accurate modeling of the surface energy balance components and thermal regime of the active layer and permafrost. A sensitivity analysis of the surface energy balance and thermal regime of the active layer and permafrost to variations in snow density and depth has been studied, the results will be presented in a forthcoming paper.

The calculated snow surface temperature and surface energy balance components must be tested against field data. Because the observed time series data for snow surface temperatures and surface energy balance components are not available, this model was validated with ground temperatures at several depths. Further studies for model validation using observational snow surface temperature and surface energy balance components are needed.

The surface energy balance approach requires large amounts of temporally evolving data, and much of which may not be available. The lack of such data limits the use of the surface energy balance model. Some local meteorological data, such as incident solar radiation, incoming longwave radiation, and atmospheric pressure, can be calculated using formulae as part of the model formulation (Liston and Hall, 1995; Liston et al., 2002), if the observed values are not available.

6. Conclusions

A one-dimensional heat transfer model with phase change, combined with a surface energy balance model, was developed to simulate surface energy balance components and permafrost temperatures. The surface energy balance equation was used to estimate the upper boundary condition for calculation of heat transfer model. The influence of unfrozen water on the physical and thermal properties of permafrost was included in the heat transfer model. The effect of snow cover was included in the combined model by extending the conduction solution into the snow layer and computing the surface heat balance and the snow surface temperature. The model presented in this study has demonstrated that the simulated soil temperatures track the measured soil temperatures quite well in the active layer, near the permafrost surface, and in shallow permafrost containing unfrozen water. Thus, the model can be used to calculate the surface energy balance components and surface temperature, and to reconstruct the temperature profile in the active layer and permafrost with a reasonable accuracy. Snow density, which determines the snow thermal conductivity, volumetric heat capacity, and albedo, can strongly affect the performance of this model.

Acknowledgements

We would like to express our gratitude to the two anonymous reviewers for their constructive and

helpful comments. We also thank Lyne Yohe who kindly edited the manuscript. This work was supported by the US National Science Foundation through the NSP OPP-9907541 and OPP-0229766, the Cooperative Institute for Arctic Research under the US National Oceanic and Atmospheric Administration (NOAA) Cooperative Agreement No. NA67RJ0147, and the China Postdoctoral Science Foundation. Financial support does not constitute an endorsement of the views expressed in this study.

References

Anderson, E.A., 1976. A point energy and mass balance model of a snow cover. NOAA Technology Report, NWS 19, p. 150.

Anderson, D.M., Tice, A.R., McKim, H.L., 1973. The unfrozen water and the apparent specific heat capacity of frozen soils. Proceedings of Second International Conference on Permafrost. National Academy of Sciences, Washington, DC, pp. 289–295.

Benson, C.S., Sturm, M., 1993. Structure and wind transport of seasonal snow on the Arctic slope of Alaska. Annals of Glaciology 18, 261–267.

Civan, F., 2000. Unfrozen water in freezing and thawing soils: kinetics and correlation. Journal of Cold Regions Engineering 14 (3), 146–156.

Civan, F., Sliepcevich, C.M., 1985. Comparison of the thermal regime for freezing and thawing of moist soils. Water Resources Research 21 (3), 407–410.

Esch, D.C., Osterkamp, T.E., 1990. Cold regions engineering: climatic concern for Alaska. Journal of Cold Regions Engineering 4 (1), 6–14.

Fleagle, R.G., Businger, J.A., 1980. An Introduction to Atmospheric Physics. Academic Press, New York, p. 432.

Goodrich, L.E., 1982. The influence of snow cover on the ground thermal regime. Canadian Geotechnical Journal 19, 421–432.

Gustafsson, D., Stahli, M., Jansson, P.E., 2001. The surface energy balance of a snow cover: comparing measurements to two different simulation models. Theoretical and Applied Climatology 70, 81–96.

Harlan, R.L., 1973. Analysis of coupled heat-fluid transport in partially frozen soil. Water Resources Research 9 (3), 1314–1323.

Hinkel, K.M., 1997. Estimating seasonal values of thermal diffusivity in thawed and frozen soils using temperature time series. Cold Regions Science and Technology 26, 1–15.

Hinkel, K.M., 2002. Soil Temperatures for Happy Valley and Barrow, Alaska. National Snow and Ice Data Center (Digital media), Boulder, CO.

Hinkel, K.M., Outcalt, S.I., Taylor, A.E., 1997. Seasonal pattern of coupled flow in the active layer at three sites in northwest North America. Canadian Journal of Earth Sciences 34, 667–678.

Hinkel, K.M., Paetzold, F., Nelson, F.E., Bockheim, J.G., 2001. Patterns of soil temperature and moisture in the active layer and upper permafrost at Barrow, Alaska: 1993–1999. Global and Planetary Change 29, 293–309.

Hinzman, L.D., Kane, D.L., Gieck, R.E., Everett, K.R., 1991. Hydrological and thermal properties of the active layer in the Alaskan arctic. Cold Regions Science and Technology 19 (2), 95–110.

Hinzman, L.D., Goering, D.J., Kane, D.L., 1998. A distributed thermal model for calculating soil temperature profiles and depth of thaw in permafrost regions. Journal of Geophysical Research 103 (D22), 28975–28991.

Inaba, H., 1983. Heat transfer behavior of frozen soil. Journal of Heat Transfer 105, 680–683.

Jame, Y.W., Norum, D.J., 1980. Hwat and mass transfer in a freezing unsaturated porous medium. Water Resources Research 16 (4), 811–819.

Johnston, G.H., Brown, R.J.E., 1964. Some observations on permafrost distribution at a lake in the Mackenzie delta, N.W.T., Canada. Arctic 17 (3), 162–175.

Jordan, R., 1991. A one-dimensional temperature model for a snow cover. CRREL Special Report, 16–91.

Kane, D.L., Hinzman, L.D., Zarling, J.P., 1991. Thermal response of the active layer to climate warming in a permafrost environment. Cold Regions Science and Technology 19, 111–122.

Kane, D.E., Hinkel, K.M., Goering, D.J., Hinzman, L.D., Outcalt, S.I., 2001. Non-conductive heat transfer associated with frozen soil. Global and Planetary Change 29, 275–292.

Kay, B.D., Goit, J.B., 1975. Temperature-dependent specific heats of dry soil material. Canadian Geotechnical Journal 12, 209–212.

Lachenbruch, A.H., 1959. Predict heat flow in a stratified medium with application to permafrost problems. U.S. Geological Survey Bulletin, 1083-A.

Lachenbruch, A.H., Marshall, B.V., 1969. Heat flow in the Arctic. Arctic 22, 300–311.

Lachenbruch, A.H., Sass, J.H., Marshall, B.V., Moses Jr., T.H., 1982. Permafrost, heat flow and the geothermal regime at Prudhoe Bay, Alaska. Journal of Geophysical Research 87 (B11), 9301–9316.

Liston, G.E., Hall, D.K., 1995. An energy balance model of lake ice evolution. Journal of Glaciology 41 (138), 373–382.

Liston, G.E., Mcfadden, J.P., Sturm, M., SR, R.P., 2002. Modeled changes in arctic tundra snow, energy and moisture fluxes due to increased shrubs. Global Change Biology 8, 17–32.

Lunardini, V.J., 1981. Heat Transfer in Cold Climates. Van Nostrand-Reinhold, New York, p. 731.

Lunardini, V.J., 1996. Climatic warming and the degradation of warm permafrost. Permafrost and Periglacial Processes 7, 311–320.

McGaw, R.W., Outcalt, S.L., Ng, E., 1978. Thermal properties and regime of wet tundra soils at Barrow, Alaska. Proceedings of the Third International Conference on Permafrost, vol. 1. National Research Council of Canada, Ottawa, pp. 48–53.

Miller, T.W., 1979. The surface heat balance in simulations of permafrost behavior. Journal of Energy Resources Technology 101 (4), 240–250.

Nakano, Y., Brown, J., 1971. Effect of a freezing zone of finite width on the thermal regime of soil. Water Resources Research 7 (5), 1226–1233.

Nakano, Y., Brown, J., 1972. Mathematical modeling and validation of the thermal regimes in tundra soils, Barrow, Alaska. Arctic and Alpine Research 4 (1), 19–28.

Ng, E., Miller, P.C., 1977. Validation of a model of the effect of

tundra vegetation on soil temperatures. Arctic and Alpine Research 9 (2), 89–104.

Osterkamp, T.E., 1987. Freezing and thawing of soils and permafrost containing unfrozen water or brine. Water Resources Research 23 (12), 2279–2285.

Outcalt, S.L., Goodwin, C., Weller, G., Brown, J., 1975. Computer simulation of the snowmelt and soil thermal regime at Barrow, Alaska. Water Resources Research 11 (5), 709–715.

Price, A.D., Dunne, T., 1976. Energy balance computations of snow melt in a sub-arctic area. Water Resources Research 12, 686–689.

Riseborough, D.H., 2002. The mean annual temperature at the top of permafrost, the TTOP model, and the effect of unfrozen water. Permafrost and Periglacial Processes 13, 137–143.

Romanovsky, V.E., Osterkamp, T.E., 2000. Effects of unfrozen water on heat and mass transport processes in the active layer and permafrost. Permafrost and Periglacial Processes 11, 219–239.

Satterlund, D.R., 1979. An improved equation for estimating longwave radiation from the atmosphere. Water Resources Research 15, 1649–1650.

Smith, M.W., Riseborough, D.H., 1983. Permafrost sensitivity to climatic change. Proceedings of 4th International Conference on Permafrost, Fairbanks, Alaska. National Academy Press, Washington, pp. 1178–1183.

Stein, J., Kane, D.E., 1983. Monitoring the unfrozen water content of soil and snow using time domain reflectometry. Water Resources Research 19, 1573–1584.

Stone, R.S., Dutton, E.G., Harris, J.M., Longenecker, D., 2002. Earlier spring snowmelt in northern Alaska as an indicator of climate change. Journal of Geophysical Research, 107 (D10) ACL10 1–15.

Sturm, M., Johson, J.B., 1991. Natural convection in the surarctic snow cover. Journal of Geophysical Research 96 (B7), 11657–11671.

Taras, B., Sturm, M., Liston, G.E., 2002. Snow-ground interface temperatures in the Kuparuk River Basin, Arctic Alaska: measurements and model. Journal of Hydrometeorology 3, 377–394.

Weller, G., Holmgren, B., 1974. The microclimates of The Arctic tundra. Journal of Applied Meteorology 13 (8), 854–862.

Williams, P.J., 1964. Unfrozen frozen water content of frozen soils and soil moisture suction. Geotechnique 14 (3), 231–246.

Williams, P.J., Smith, M.W., 1989. The Frozen Earth: Fundamentals of Geocryology. Cambridge Univ. Press, Cambridge, p. 306.

Zhang, T., Stamnes, K., 1998. Impact of climatic factors on the active layer and permafrost at Barrow, Alaska. Permafrost and Periglacial Processes 9, 229–246.

Zhang, T., Osterkamp, T.E., Stamnes, K., 1996. Influence of the depth hoar layer of the seasonal snow cover on the ground thermal regime. Water Resources Research 32 (7), 2075–2086.

Zhang, T., Barry, R.G., Haeberli, W., 2001. Numerical simulation of the influence of the seasonal snow cover on the occurrence of permafrost at high latitudes. Norsk Geografisk Tidsskrift 55, 261–266.